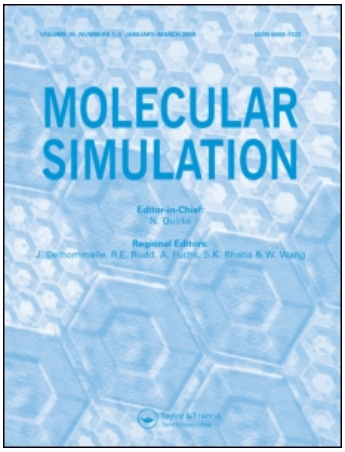


**Molecular Simulation**
Publication details, including instructions for authors and subscription information:
http://www.informaworld.com/smpp/title~content=t713644482

# Simulation of phase transitions via spatial updating and tempering

Daniel P. Noon[a]; G. Orkoulas[a]
[a] Department of Chemical and Biomolecular Engineering, University of California, Los Angeles, CA, USA

Online publication date: 03 August 2010

**To cite this Article** Noon, Daniel P. and Orkoulas, G.(2010) 'Simulation of phase transitions via spatial updating and tempering', Molecular Simulation, 36: 7, 535 — 543
**To link to this Article: DOI:** 10.1080/08927021003671574
**URL:** http://dx.doi.org/10.1080/08927021003671574

*Molecular Simulation*
Vol. 36, Nos. 7–8, June–July 2010, 535–543

Taylor & Francis
Taylor & Francis Group

# Simulation of phase transitions via spatial updating and tempering

Daniel P. Noon and G. Orkoulas*

*Department of Chemical and Biomolecular Engineering, University of California, Los Angeles, CA 90095, USA*

(*Received 1 November 2009; final version received 2 February 2010*)

In spatial updating grand canonical Monte Carlo, the elementary moves are implemented either by selecting points in space at random (random updating) or in a predetermined order (sequential updating). Previous work indicates that spatial updating is more efficient than standard updating and is ideal for parallel processing via domain decomposition. In this work, it is shown that the combination of spatial updating grand canonical Monte Carlo with tempering techniques can increase the simulation efficiency of phase transitions by several orders of magnitude. In simulated tempering, several macrostates are coupled together to form a super-ensemble or an expanded ensemble. Each macrostate comprises a grand canonical system at a given value of the chemical potential and the temperature. The elementary steps consist of particle transfers as well as switches between different macrostates. The switches can be implemented according to a Metropolis or a heat-bath algorithm. The combination of spatial updating with tempering is used in the investigation of the vapour–liquid transition of the 2D Lennard-Jones fluid. The critical parameters are estimated from finite-size scaling techniques using a Landau expansion of the free energy density. In the near-critical region, the efficiency enhancement is two to four orders of magnitude higher than conventional algorithms. The increased efficiency and the feasibility of parallel processing allows for simulations of much larger systems than is possible with standard algorithms.

**Keywords:** Monte Carlo; phase transitions; tempering; parallel processing



## 1. Introduction

Spatial updating grand canonical Monte Carlo algorithms [1,2] are generalisations of random and sequential updating algorithms for lattice systems to continuum fluid models. The elementary steps, insertions and removals, are constructed by generating points in space, either at random (random updating) or in a predefined order (sequential updating). The type of move is deduced by examining the local environment in the neighbourhood of the selected point. Due to the nature of the updating, spatial updating is more efficient than standard grand canonical updating [3,4] and is ideal for parallel implementation via domain or geometric decomposition techniques [2].

Exploration of the critical region in simulations is difficult due to the unbounded growth of correlations and fluctuations in the vicinity of the critical point. These slowing down effects are responsible for long relaxation times and cause the simulations to slow down substantially. For systems characterised by special particle–hole symmetries such as magnetic Ising and lattice gas systems, significant progress has been made in developing cluster type of techniques [5,6] capable of reducing critical slowing down effects. These techniques, however, cannot be easily extended into asymmetric off-lattice continuum fluid models.

In a similar perspective, simulation of highly subcritical temperatures encounters difficulties due to tunnelling effects associated with high free energy barriers separating local free energy minima that correspond to stable coexisting phases. States of high free energy are intermediate to those of the pure phases and typically consist of a mixture of the two phases separated by interfaces. Since the free energy penalty associated with interface formation is high, these intermediate states have low probability of occurrence. Similar problems are also encountered in systems of rough free energy landscapes that consist of many local minima separated by high free energy barriers. Depending on the temperature and the simulated system size, conventional simulations may get trapped in one of these local minima. Standard techniques must be modified such that the intermediate configurations are sampled just as often as the stable phases.

Simulation techniques that enhance the otherwise infrequent transitions between the two coexisting phases are generally referred to as flat-histogram techniques. They execute a nearly uniform random walk in terms of an appropriate order parameter via a suitable modification of the sampling distribution. The most common of these techniques are multicanonical [7], entropic [8] and Wang–Landau [9] type of sampling. In the context of a grand canonical type of updating, the previous techniques traverse a uniform random walk in terms of the density and/or the energy. Another class of flat-histogram type of methods, commonly referred to as tempering methods

*Corresponding author. Email: makis@seas.ucla.edu

ISSN 0892-7022 print/ISSN 1029-0435 online

DOI: 10.1080/08927021003671574
http://www.informaworld.com

[10–13], comprises uniform random walks in terms of the field variables, i.e. temperature and chemical potential for the case of grand canonical sampling.

In this work, the vapour–liquid transition of the 2D Lennard-Jones fluid is investigated via spatial updating grand canonical Monte Carlo simulations. In order to overcome the infrequent transitions between the two coexisting densities, these simulations are implemented in conjunction with tempering techniques. In simulated tempering [10,11], several macrostates (or replicas) are combined to form a super-ensemble or an expanded ensemble. Each macrostate comprises a grand canonical system at fixed values of the chemical potential and the temperature. The elementary steps consist of particle transfers as well as transitions between different macrostates. The switches between different macrostates can be implemented according to a Metropolis or a heat-bath [14] algorithm. The simulation results indicate that the heat-bath algorithm is more efficient than the Metropolis algorithm for a modest number of switching attempts.

In order to simulate vapour–liquid transitions through a grand canonical type of updating, one must construct a line that approximates the phase boundary in the space of the chemical potential and the temperature. In this work, the macrostates are selected from the maximum compressibility line, covering a range of temperatures that correspond to both single- and two-phase systems. The critical parameters are estimated from finite-size scaling techniques using a Landau expansion of the size-dependent free energy density. Since the efficiency enhancement is two to four orders of magnitude in the near-critical region, much larger systems can be simulated than is possible with conventional algorithms. For large systems, the simulations are implemented in parallel through decomposition techniques into a number of non-interacting domains.

## 2. Spatial updating and tempering

Consider a grand canonical system of indistinguishable particles of diameter $\sigma$ in a $d$-dimensional volume $V$ at temperature $T$. The particles interact according to a pair-wise additive potential, e.g. Lennard-Jones. Suppose that the current configuration contains $N$ particles at positions $\mathbf{r}_1, \mathbf{r}_2, \ldots, \mathbf{r}_N$. In spatial updating [1,2], a uniform random point, $\mathbf{r}$, is generated within the simulation volume $V$. If $|\mathbf{r} - \mathbf{r}_n| > \sigma/2 \ \forall n = 1, 2, \ldots, N$, particle insertion is attempted and the position of the particle is obtained at random within a $d$-dimensional sphere of diameter $\sigma$. Particle removal is attempted when there is only one particle, say $m$, for which $|\mathbf{r} - \mathbf{r}_m| \leq \sigma/2$ and $|\mathbf{r} - \mathbf{r}_n| > \sigma/2 \ \forall n \neq m$. For these two cases, the acceptance probability, $\alpha_{ij}$, from state $i$ that contains $N$ particles to state $j$ that contains $N \pm 1$ particles, is given by [1,2]:

$$\alpha_{ij} = \min\{1, (zv)^{\pm 1} \exp(-\beta \Delta U)\}, \tag{1}$$

where $(+)$ corresponds to insertion and $(-)$ to removal. In Equation (1), $\Delta U$ is the potential energy difference between states $i$ and $j$, $v$ is the volume of a $d$-dimensional sphere with diameter $\sigma$ and $\beta = 1/k_B T$, where $k_B$ is Boltzmann's constant. The activity, $z$, of the particles is defined as $z = \Lambda^{-d} \exp(\beta\mu)$, where $\mu$ is the chemical potential and $\Lambda$ is the thermal De Broglie wavelength. The case for which $|\mathbf{r} - \mathbf{r}_m| \leq \sigma/2$ for more than a single particle corresponds to double (or multiple) overlaps. In such a case, the proposed update is rejected and the current state is counted again. Simulation results on 2D and 3D Lennard-Jones systems [2] indicate that the rejection scheme associated with double/multiple overlaps does not affect sample quality.

A 2D illustration of the type of spatial updating that is used in this work is shown in Figure 1. Since closed-packed configurations in two dimensions correspond to hexagonal type of particle arrangements, the total area is divided into $n^2$ hexagons of area $\sqrt{3}\sigma^2/2$ and side $\sqrt{3}\sigma/3$, where $\sigma$ is the particle diameter and $n$ is an integer. The centre of a hexagon from the centres of its six neighbouring hexagons is thus $\sigma$. The dimensions of the simulation box are $L_x = n\sigma$ and $L_y = \sqrt{3}L_x/2$

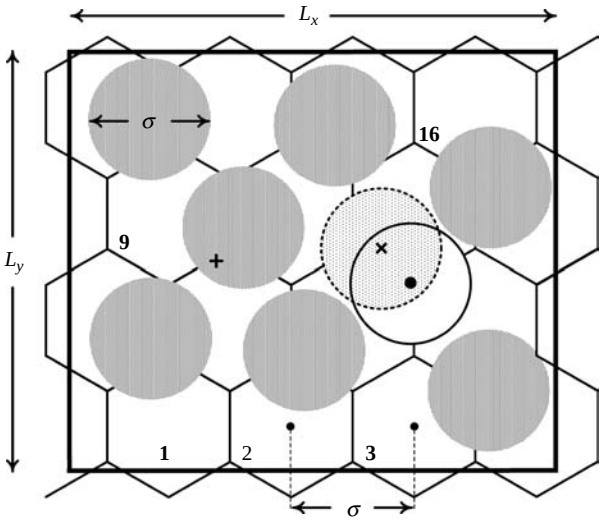


Figure 1. 2D illustration of the methodology of spatial updating. The simulation area consists of $n^2$ hexagons of area $\sqrt{3}\sigma^2/2$ and side $\sqrt{3}\sigma/3$, where $\sigma$ is the particle diameter and $n$ is an integer. The dimensions of the simulation box are $L_x = n\sigma$ and $L_y = \sqrt{3}L_x/2$. Points are generated either at random (random updating) or according to a predefined order (sequential updating). Point '+' corresponds to particle removal while point '×' to particle insertion. The position of the particle, shown as '•', is obtained at random within a circle of diameter $\sigma$ centred at point '×'.

(see Figure 1). Random updating corresponds to generating points at random with uniform probability within the simulation area $L_xL_y$. In Figure 1, point ' + ' corresponds to particle removal while point ' × ' to particle insertion. For the case of insertion, the position of the particle (shown as '•' in Figure 1) is obtained at random within a circle of diameter $\sigma$ centred at point ' × ' as shown in Figure 1. In sequential updating, the $n^2$ hexagons are labelled in a definitive order, i.e. in terms of rows as shown in Figure 1. A random point, **r**, is then generated with uniform probability in a hexagon. Sequential updating corresponds to implementing spatial updating at point **r** in hexagon $J$ in the order $J = 1, 2, \ldots, n^2$. After the completion of these $n^2$ updates, another random point, **r**, is generated and the process is repeated. The choice of the simulation area shown in Figure 1 is not unique. Alternatively, a square simulation box of $n^2$ cells of side $\sigma$ could be considered, as was done in previous work [1,2]. The particular choice of the simulation area shown in Figure 1 does not affect the results when only disordered phases are of interest. However, it is of crucial importance in simulation of crystal phases (e.g. [15]).

In conventional grand canonical Monte Carlo simulations [3,4], the elementary updates often consist of particle transfers (insertions and removals) and particle displacements. The nature of the move (transfer vs. displacement) is decided with a fixed probability. However, particle displacements are not necessary since insertions and removals cause energy fluctuations also. In this work, particle displacements are not considered.

In this work, the sequential version of the grand canonical technique of spatial updating is used in conjunction with tempering methodologies in order to overcome tunnelling effects associated with simulation of two-phase coexistence. According to simulated tempering [10,11], $K$ macrostates (or replicas) are coupled to form a super-ensemble or an expanded ensemble with partition function $Z$ defined as follows:

$$Z = \sum_{m=1}^{K} \Xi_m \, \mathrm{e}^{\eta_m}. \tag{2}$$

Macrostate $m$ ($m = 1, 2, \ldots, K$) corresponds to a grand canonical system at temperature $T = T_m$ (or inverse temperature $\beta = \beta_m$) and chemical potential $\mu = \mu_m$ (or activity $z = z_m$). In Equation (2), $\Xi_m = \Xi(\mu_m, V, T_m)$ is the grand partition function at temperature $T_m$ and chemical potential $\mu_m$. $\eta_m$ is a weighting factor associated with macrostate $m$.

Inspection of the partition function $Z$ in Equation (2) indicates that two types of moves are possible: particle transfers and transitions between the $K$ macrostates. Particle transfers are implemented according to spatial updating and accepted using Equation (1) with $z = z_m$ and $\beta = \beta_m$. The transitions between the $K$ grand canonical systems can either be implemented according to a Metropolis or a heat-bath type of algorithms. For a state of $N$ particles with total potential energy $U$, the Metropolis acceptance probability from ($T_m$, $\mu_m$) to ($T_n$, $\mu_n$) is given by

$$\alpha_{mn} = \min\left\{1, \exp\left[N \ln\left(\frac{z_n}{z_m}\right) - \Delta\beta \cdot U + \Delta\eta\right]\right\}, \tag{3}$$

where $\Delta\beta = \beta_n - \beta_m$ and $\Delta\eta = \eta_n - \eta_m$. Alternatively, a heat-bath type of algorithm may be used [14]. In such a case, the transition probability, $P_{mn}$, from ($T_m$, $\mu_m$) to ($T_n$, $\mu_n$) is given by

$$P_{mn} = \frac{z_n^N \mathrm{e}^{-\beta_n U + \eta_n}}{\sum_{r=1}^{K} z_r^N \mathrm{e}^{-\beta_r U + \eta_r}}. \tag{4}$$

The weighting factors $\eta_m$ control the frequency with which these $K$ macrostates are visited in the course of the simulation. From Equation (2), it follows that the probability, $\pi_m$, of observing the $m$th macrostate, irrespective of the particular microscopic configuration, is

$$\pi_m = \frac{1}{Z} \Xi_m \, \mathrm{e}^{\eta_m}. \tag{5}$$

The weighting factors $\eta_m$ must be chosen such that $\pi_m$ are of the same order of magnitude. If $F_m = \ln \Xi_m$ is the grand potential (free energy) at $T = T_m$ and $\mu = \mu_m$, the choice $\eta_m = -F_m$ renders $\pi_m = \text{const.}$ $\forall m$, i.e. each macrostate is visited with the same frequency. Since the free energies $F_m$ are unknown, an iterative procedure is required during which the weights are refined until the resulting distribution $\pi_m$ is nearly flat.

## 3. Convergence analysis

The previous algorithms were tested for the 2D Lennard-Jones fluid. The Lennard-Jones pair potential, $\phi_{\mathrm{LJ}}(r)$, is defined as:

$$\phi_{\mathrm{LJ}}(r) = 4\varepsilon\left[\left(\frac{\sigma}{r}\right)^{12} - \left(\frac{\sigma}{r}\right)^{6}\right], \tag{6}$$

where $r$ is the distance between two particles of diameter $\sigma$, and $\varepsilon > 0$ is the depth of the potential in units of energy. For computational simplicity, the pair potential is truncated at a distance $r = \lambda\sigma$, i.e.

$$\phi(r) = \begin{cases} \phi_{\mathrm{LJ}}(r), & r \le \lambda\sigma, \\ 0, & r > \lambda\sigma, \end{cases} \tag{7}$$

where $\lambda = 3$. The system can be described by the reduced temperature $T^* = k_{\mathrm{B}}T/\varepsilon$, the reduced activity $z^* = z\sigma^2$

and the reduced density $\rho^* = (2/\sqrt{3})N(\sigma/L_x)^2$, where $N$ is the fluctuating number of particles and $L_x = n\sigma$.

In order to investigate the efficiency of spatial updating and tempering, a total of 36 different values of $\mu$ were considered along the isotherm that corresponds to a reduced temperature of $T^* = 0.535$ for a system size of $L_x = 20\sigma$. These 36 values of $\mu$ on the $T^* = 0.535$ isotherm are shown in Figure 2. The simulation time, $t$, is measured in sweeps where one sweep corresponds to $n^2 = 400$ elementary steps that consist of particle transfers and switching attempts between different values of $\mu$, i.e. different macrostates. A single simulation covers a wide range of densities, $0.1 \lesssim \rho^* \lesssim 0.6$. The weighting factors $\eta_m$ were estimated from previous work [2]. The efficiency may be inferred from measurements of autocorrelation functions defined as

$$\Phi(t) = \frac{\langle X(0)X(t)\rangle - \langle X\rangle^2}{\langle X^2\rangle - \langle X\rangle^2}, \tag{8}$$

where $X$ is a fluctuating variable (i.e. density). The integrated relaxation time, $\tau$, defined as

$$\tau = \int_0^\infty \mathrm{d}t\, \Phi(t), \tag{9}$$

is a measure of the number of sweeps required to generate a statistically independent configuration.

Results for the relaxation time, $\tau$, obtained from the density autocorrelation functions are shown in Figure 3. The two topmost curves correspond to 36 independent simulations with conventional and spatial updating. As it has been seen and explained in previous work [1,2], spatial updating is more efficient than standard updating. However, Figure 3 indicates that the combination of spatial updating and tempering results in additional efficiency enhancement compared to independent simulations. The remaining four curves in Figure 3 correspond to results obtained from a single simulation with a Metropolis tempering algorithm (cf. Equation (3)). In these simulations, the elementary steps are executed sequentially: a number of spatial updates are implemented followed by an attempt to switch to a different value of $\mu$. The crucial parameter that controls efficiency is the frequency of switches between different macrostates. The autocorrelation time decreases substantially as the frequency of transitions increases. A frequent number of switching attempts force the system to decorrelate much faster. A simulation for which the transitions between different macrostates are not so frequent roughly corresponds to implementing independent simulations, and the concomitant reduction of $\tau$ is thus very small.

As already commented, the transitions between different grand canonical systems can either be implemented according to a Metropolis, Equation (3), or a heat-bath algorithm, Equation (4). A comparison between these two algorithms is shown in Figure 4 for $\ln(z^*) = -3.045$. This particular value of the activity is the inflection point of the isotherm of Figure 2, which roughly corresponds to the maximum of the curves of

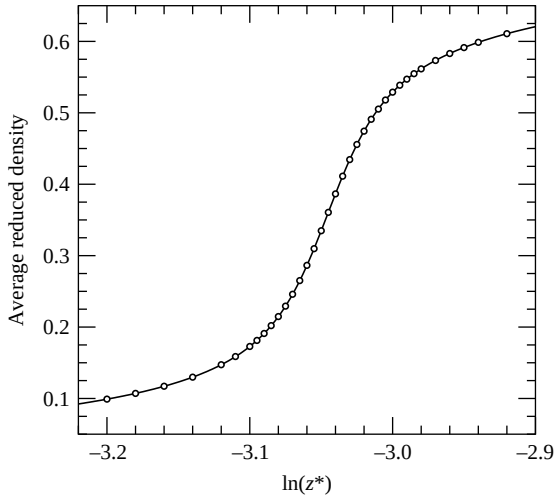


Figure 2. Average reduced density, $\langle\rho^*\rangle$ vs. reduced activity, $z^* = z\sigma^2$, for the 2D Lennard-Jones fluid at $T^* = 0.535$ and $L_x = 20\sigma$ obtained from grand canonical Monte Carlo simulations with spatial updating and tempering. A single simulation corresponds to a random walk over 36 different values of $\mu$, shown as circles (◦). The solid line has been obtained via histogram reweighting [16,17] techniques.

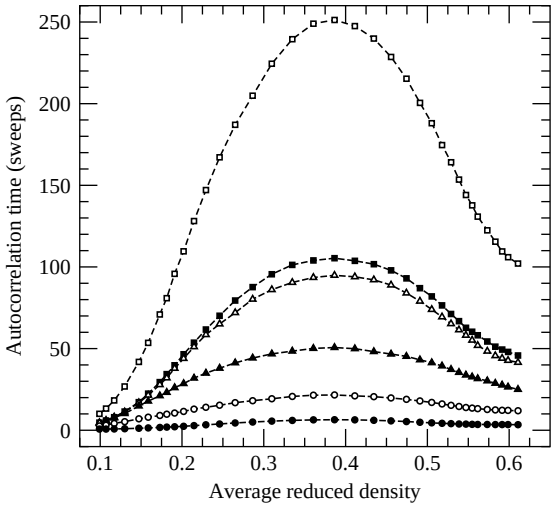


Figure 3. Integrated autocorrelation time, $\tau$, as a function of the average reduced density, $\langle\rho^*\rangle$, for the 2D Lennard-Jones fluid at $T^* = k_B T/\varepsilon = 0.535$ and $L_x = 20\sigma$. The two topmost curves correspond to 36 independent simulations with conventional (□) and spatial (■) updating, respectively. The remaining curves correspond to single simulations with a Metropolis tempering algorithm. From the third curve from the top, respectively, the switch frequency is: 1000 sweeps (△), 100 sweeps (▲), 10 sweeps (◦) and 0.1 sweeps (•).

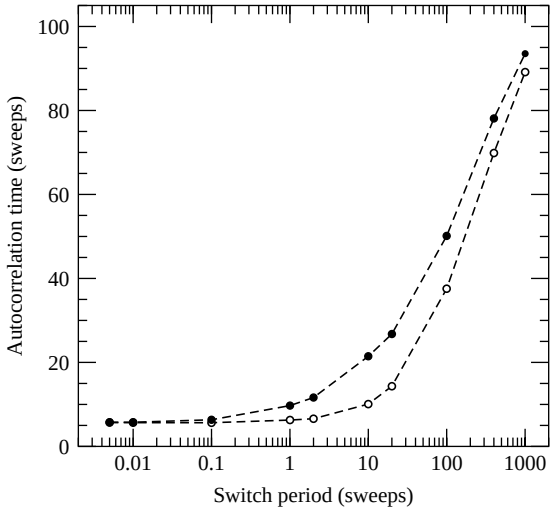


Figure 4. Relaxation time, $\tau$, as a function of the tempering switch period for the 2D Lennard-Jones fluid at $T^* = k_B T/\varepsilon = 0.535$, $\ln(z^*) = \ln(z\sigma^2) = -3.045$ and $L_x = 20\sigma$. Shown are results for the heat-bath (◦) and Metropolis (•) algorithms.

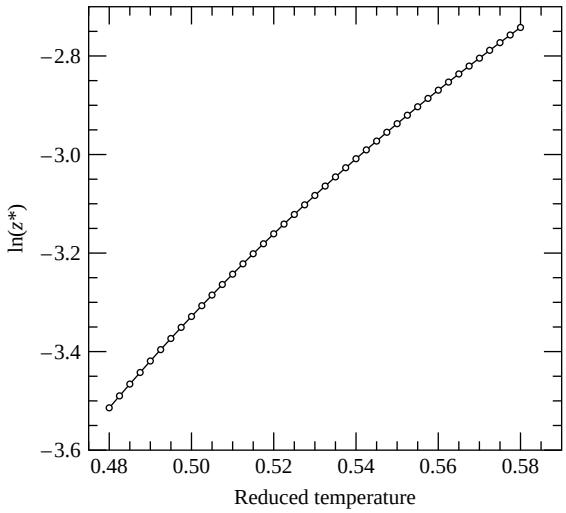


Figure 5. The set of 41 macrostates, shown by (◦), that was used in the investigation of the vapour–liquid transition of the 2D Lennard-Jones system. These macrostates were determined by locating the value of $\mu$ that corresponds to the maximum compressibility for a given temperature. The calculations were implemented by analysing the data of Figure 2 through histogram reweighting techniques. Solid line is drawn for visual clarity.



Figure 3. As can also be seen from Figure 3, the autocorrelation time, $\tau$, decreases substantially as the tempering frequency increases. When the tempering frequency becomes comparable to the frequency of the grand canonical updates, both algorithms are equivalent in terms of efficiency. Otherwise, the heat-bath algorithm is slightly more efficient than the Metropolis algorithm.

## 4. Location of the critical point

This section is associated with the location of the critical temperature, $T_c$, and activity, $z_c$, of the 2D Lennard-Jones fluid using spatial updating and tempering. A single simulation should visit a sufficient number of macrostates representative of single- and two-phase systems. For magnetic Ising and lattice gas models, the phase boundary and its analytic extension in the single-phase region coincide with the axis of symmetry. For continuum fluid models, however, the phase boundary must be established from the simulations. Thus, one must construct a line that approximates the phase boundary and its extension in the single-phase region. A simple choice comprises the line of inflection points of the density vs. chemical potential isotherms which corresponds to the maximum of the susceptibility (or compressibility) defined as $\chi = (\partial\rho/\partial\mu)_T$. The choice of this pseudo-symmetry axis is not unique and other possibilities also exist (e.g. [18]).

Using the data for $T^* = 0.535$ and $L_x = 20\sigma$, the line of maximum susceptibility was estimated in the $\mu - T$ plane through histogram reweighting [16,17]. The result of this construction is shown in Figure 5. A total of 41 macrostates were considered on this line. These states correspond to reduced temperatures $T^* = 0.4800$, $0.4825, \ldots, 0.5775, 0.5800$ (see Figure 5), and they cover both high-$T$ single-phase and low-$T$ two-phase systems. A single simulation utilising spatial updating and tempering visits all 41 macrostates with nearly uniform probability. Simulations were implemented for system sizes $L_x = n\sigma$, with $n = 10, 12, 16, 20, \ldots, 56, 60$. An initial set of weights, $\eta_m$, were estimated from the simulations at $T^* = 0.535$, as shown in Figure 2. These weights were refined accordingly, as more data from the states shown in Figure 5 became available. The simulations were implemented in sweeps, where one sweep comprises $n^2$ elementary steps. The switch frequency between different macrostates was set to 0.25 sweeps and implemented via a heat-bath algorithm.

For system sizes $L_x \geq 40\sigma$, the simulations were implemented in parallel via domain decomposition techniques. As it was explained in previous work [2], the sequential version of spatial updating can be implemented in parallel in $p > 1$ processors by dividing the simulation volume (area) into $p$ domains. Each processor updates its own domain independently of the other processors. It is important to emphasise that the type of parallel processing employed in this work is only applicable to systems for which the intermolecular potential is of finite range. The efficiency of parallel processing depends on the frequency of information exchange between logically adjacent processor which is, usually, a slow process. For a given system size, the efficiency vs. number of processor curve

typically exhibit a minimum that defines the optimal number of processors (e.g.[2,19]). In this work, the optimal number of processors was found by measuring the execution time vs. number of processors through short simulations. Once a nearly optimal value for the number of processors was established, a long simulation was executed to collect statistics. The parallel simulations were implemented on Intel Xeon processors and the communications were implemented via message passing interface (MPI). Parallel simulations for $L_x \geq 60\sigma$ were not attempted since the optimal number of processors exceeded the number of available processors, thus rendering parallel processing impractical.

Using the data for a given $L_x$, one may obtain $L$-dependent values for the critical temperature and chemical potential and extrapolate towards the thermodynamic limit using finite-size scaling techniques. According to finite-size scaling theory [20,21], a quantity $F$, which exhibits a power-law type of divergence in the thermodynamic limit,

$$F \sim |t|^{-\omega}, \text{ with } t = \frac{T - T_c}{T_c}, \tag{10}$$

is expected to scale asymptotically as

$$F(t, L) \approx L^{\omega/\nu} \tilde{F}(tL^{1/\nu}), \tag{11}$$

in the limit of large $L$. In Equation (11), $\nu$ is the exponent that describes the divergence of the correlation length and $\tilde{F}$ is a universal scaling function. The scaling from of Equation (11) implies that $F$ will reach a maximum (or minimum) of height proportional to $L^{\omega/\nu}$. The location of the extremum, which may be regarded as an effective, $L$-dependent critical temperature, $T_c(L)$, scales with $L$ as

$$T_c(L) - T_c(\infty) \sim L^{-1/\nu}, \tag{12}$$

where $T_c(\infty)$ is the critical temperature in the limit of infinite system size.

Given Monte Carlo simulations for a series of system sizes $L$, the critical point may be obtained by measuring second- and higher-order derivatives of the grand potential in terms of appropriate density–energy moments [18], locating the $L$-dependent peak positions, and extrapolating in the limit of infinite size via Equation (12). In this work, a simpler procedure based on analysing a Landau type of expansion of the free energy density is used. This procedure has the advantage of yielding $L$-dependent critical parameters that approach their infinite-size analogues from *above*, thus avoiding the need to implement expensive simulations at very low temperatures. Using histogram reweighting techniques [16,17], the $L$-dependent grand canonical distribution of densities, $P_L(\rho; T, \tilde{\mu})$, may be constructed for a given value of temperature, $T$, and chemical potential, $\tilde{\mu} = \ln(z\sigma^2)$. The canonical free energy density, $f_L(T, \rho)$, is related to $P_L(\rho; T, \tilde{\mu})$ via

$$\ln P_L(\rho; T, \tilde{\mu}) \propto -f_L(T, \rho)V + \tilde{\mu}N, \tag{13}$$

where $V$ is the volume (area). An $L$-dependent canonical free energy density may thus be extracted from the data via Equation (13). Since, for a finite system, analyticity is anticipated, $f_L$ may be fitted to a Landau type of expansion [18]

$$f_L(T, \rho) = \sum_{j=0}^{J} A_j(T; L)\rho^j, \tag{14}$$

where $J \geq 4$. The critical point may be found from $\partial^2 f_L/\partial\rho^2 = \partial^3 f_L/\partial\rho^3 = 0$, which corresponds to the vanishing of the inverse susceptibility.

The $L$-dependent free energy density, $f_L$, was obtained for $10\sigma \leq L_x \leq 60\sigma$ in terms of $\rho$ and $T$ using histogram reweighting. The central portion ($0.25 \lesssim \rho^* \lesssim 0.50$) was fitted to the Landau form, Equation (14), with $J = 4$. Fitting the whole function to its Landau form, Equation (14), would require $J > 4$ Landau coefficients $A_j$. The $L$-dependent values for the critical temperature, $T_c(L_x)$, and chemical potential, $\tilde{\mu}_c(L_x)$, so obtained were extrapolated to the limit of infinite size according to Equation (12) using $\nu = 1$ appropriate for 2D Ising criticality [22]. The extrapolation of the effective critical parameters towards the limit of infinite size is shown in Figures 6 and 7. In order to minimise non-linearities associated with correction-to-scaling terms [23], the data that correspond to small systems ($L_x \leq 20\sigma$) were excluded from the fit. The data conform to a linear fit with satisfactory precision and yield $T_c^*(\infty) = 0.4879(3)$, $\tilde{\mu}_c^*(\infty) = -3.422(2)$. The error is due to the small scatter of the measured $L$-dependent data points.

Using the critical temperature found from Figure 6 and the critical value of $\tilde{\mu}$ from Figure 7, histogram reweighting was performed on each of these simulations to determine the critical value for the mean density for each system size $L_x$. The best estimate for the density at the critical point was taken to be the average value of the densities found through reweighting, along with some uncertainty. The value of $\langle\rho^*\rangle_c = 0.363 \pm 0.004$ was the result of this computation.

A comparison of the relaxation time for simulations with and without tempering is shown in Figure 8. The filled circles are the relaxation time for the macrostate that corresponds to the lowest temperature in Figure 5, i.e. $T^* = 0.48$ and $\tilde{\mu} = \ln(z\sigma^2) = -3.51416$. The open circles correspond to conventional grand canonical simulations without tempering at the same values of $T$ and $\mu$. Clearly, the combination of spatial updating with tempering offers an efficiency enhancement which is several orders of magnitude higher than conventional

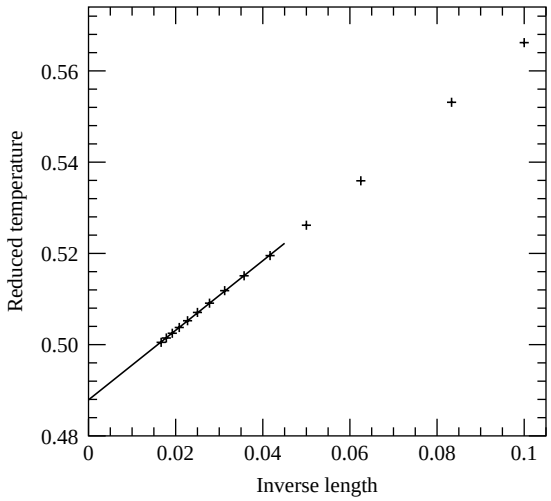


Figure 6. Critical temperature estimation for the 2D Lennard-Jones fluid. The $L$-dependent critical temperatures, $T_c^*(L_x)$, shown by crosses ( $\times$ ) are obtained from a Landau expansion of the canonical free energy density as explained in the text. The effective critical temperatures are plotted vs. $(L_x/\sigma)^{-1/\nu}$, where $\nu = 1$. The solid line is a linear fit. The data that correspond to $L_x \leq 20\sigma$ are excluded from the fit. The intersection of the solid line with the ordinate defines $T_c^*(\infty)$.

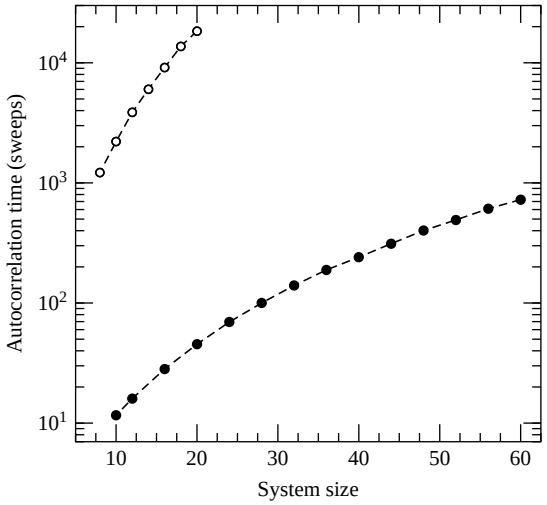


Figure 8. Relaxation time, $\tau$, vs. system size, $L_x$, for the 2D Lennard-Jones fluid at $T^* = 0.480$ and $\tilde{\mu} = \ln(z\sigma^2) = -3.51416$. The open circles ($\circ$) correspond to grand canonical simulations with standard updating. The filled circles ($\bullet$) are results from spatial updating with tempering.

algorithms. Figure 8 indicates that it is impractical to simulate system sizes $L_x > 20\sigma$ with conventional updating since the relaxation time grows enormously. It may be argued that a combination of conventional updating with tempering could result in a performance better than the results, shown by open circles, in Figure 8. As the system size increases, however, the execution time also increases, which, in fact, renders serial simulations notoriously long in terms of wall-clock time. The key factor that allows for simulation of large systems is the parallelisation option of spatial updating via domain decomposition. As already emphasised, the simulations for $L_x \geq 40\sigma$ were implemented in parallel using the optimal number of processors that yields maximum parallel efficiency. Although it is possible to simulate system sizes $L_x \geq 60\sigma$, it was not attempted here due to limitations in the maximum number of available processors.

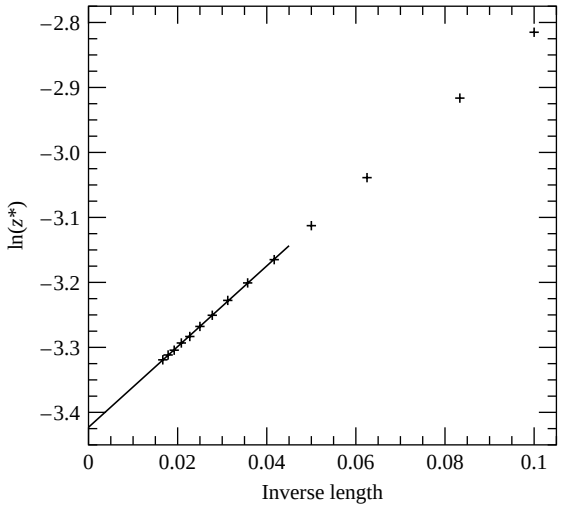


Figure 7. Estimation of the critical value of the chemical potential, $\tilde{\mu} = \ln(z\sigma^2)$, for the 2D Lennard-Jones fluid. The procedure is analogous to that of Figure 6.

## 5. Discussion and conclusions

Open types of ensembles (e.g. grand canonical), in which both the energy and the density fluctuate, are very convenient in numerical studies of phase transitions. However, as system complexity increases, improved algorithms that facilitate transitions between different microscopic configurations are required. The main contributing factor for reducing autocorrelation time in spatial updating grand canonical Monte Carlo lies in the way by which the elementary steps are implemented. Rather than a priori deciding on either insertion or removal, the elementary step in spatial updating is deduced based on the local environment of a point in space. If the sequence of point is selected appropriately, spatial correlations among particles may be reduced and enhancement may be obtained. In addition, due to the nature of the updating, spatial updating is ideal for parallel implementation via domain decomposition techniques. The spatial updating scheme

of Figure 1 can be further enhanced using collective updating moves for lattice systems [5,6], configurational-bias methods [24–26] for polymer systems and distance-bias techniques [27,28] for electrolyte solutions.

Investigation of first- and second-order phase transitions via molecular simulations is difficult due to the unbounded growth of correlations and fluctuations in the critical region and due to tunnelling effects associated with crossing high free energy barriers separating stable coexisting phases. In this work, it is shown that a combination of spatial updating grand canonical Monte Carlo with tempering techniques can increase the simulation efficiency by several orders of magnitude compared to standard algorithms. The increased efficiency and the possibility of parallel implementation allows for simulations of much larger systems than is currently possible with conventional algorithms. Indeed, given enough independent processors, a resolution similar to that achieved for ferromagnetic Ising models [29] may be attained.

In tempering techniques, the transition probability between different macrostates or replicas is very sensitive to the number of replicas as well as their spacing. The number of replicas also controls the total execution time, i.e. wall-clock time. The increase of the total execution time places a practical upper bound on the maximum number of replicas. In this work, the maximum number of replicas was set to 36 (Figure 2) and 41 (Figure 5) due to CPU time limitations and no attempt was made to optimise the number and spacing of the replicas. Although significant theoretical work has been invested [30–32] in devising an optimal spacing (such as geometric type of progressions) of the $K$ macrostates or replicas in tempering techniques, the CPU requirements are roughly expected to increase by a factor of $K$ compared to simulations of a single replica. Moreover, as the system size increases, the acceptance probability associated with transitions between different macrostates decreases. Thus, for simulations of very large systems, additional replicas may have to be considered with a concomitant increase of the total execution time. Hence, the feasibility of parallel processing is crucial for the success of tempering methods.



## Acknowledgements

The authors are grateful to the Intel Higher Education Program, which provided the Linux cluster used in the simulations. The authors are also grateful to the developers of MPICH at Argonne National Laboratory, which made parallel programming of this work convenient and possible. Financial support from NSF, CBET-0652131 and CBET-0967291 is gratefully acknowledged.

## References

[1] G. Orkoulas, *Acceleration of Monte Carlo simulations through spatial updating in the grand canonical ensemble*, J. Chem. Phys. 127 (2007), pp. 084106-1–084106-9.
[2] C.J. O'Keeffe, R. Ren, and G. Orkoulas, *Spatial updating grand canonical Monte Carlo algorithms for fluid simulation: Generalization to continuous potentials and parallel implementation*, J. Chem. Phys. 127 (2007), pp. 194103-1–194103-8.
[3] G.E. Norman and V.S. Filinov, *Investigations of phase transitions by a Monte Carlo method*, High Temp. (USSR) 7 (1969), pp. 216–222.
[4] D.J. Adams, *Grand canonical ensemble Monte Carlo for a Lennard-Jones fluid*, Mol. Phys. 29 (1975), pp. 307–311.
[5] R.H. Swendsen and J.-S. Wang, *Nonuniversal critical dynamics in Monte Carlo simulations*, Phys. Rev. Lett. 58 (1987), pp. 86–88.
[6] U. Wolff, *Collective Monte Carlo updating for spin systems*, Phys. Rev. Lett. 62 (1989), pp. 361–364.
[7] B.A. Berg and T. Neuhaus, *Multicanonical ensemble: A new approach to simulate first-order phase transitions*, Phys. Rev. Lett. 68 (1992), pp. 9–12.
[8] J. Lee, *New Monte Carlo algorithm: Entropic sampling*, Phys. Rev. Lett. 71 (1993), pp. 211–214.
[9] F. Wang and D.P. Landau, *Efficient multiple-range random walk to calculate the density of states*, Phys. Rev. Lett. 86 (2001), pp. 2050–2053.
[10] E. Marinari and G. Parisi, *Simulated tempering: A new Monte Carlo scheme*, Europhys. Lett. 19 (1992), pp. 451–458.
[11] A.P. Lyubartsev, A.A. Martinovski, S.V. Shevkunov, and P.N. Vorontsov-Velyaminov, *New approach to Monte Carlo calculation of the free energy: Method of expanded ensembles*, J. Chem. Phys. 96 (1992), pp. 1776–1783.
[12] R.H. Swendsen and J.-S. Wang, *Replica Monte Carlo simulation of spin glasses*, Phys. Rev. Lett. 75 (1986), pp. 2607–2609.
[13] K. Hukushima and K. Nemoto, *Exchange Monte Carlo method and application of spin glass simulations*, J. Phys. Soc. Jpn. 65 (1996), pp. 1604–1608.
[14] D.P. Landau and K. Binder, *A Guide to Monte Carlo Simulations in Statistical Physics*, Cambridge University Press, Cambridge, 2000.
[15] G. Orkoulas and D.P. Noon, *Spatial updating in the great grand canonical ensemble*, J. Chem. Phys. 131 (2009), pp. 161106-1–161106-4.
[16] A.M. Ferrenberg and R.H. Swendsen, *New Monte Carlo technique for studying phase transitions*, Phys. Rev. Lett. 61 (1988), pp. 2635–2638.
[17] A.M. Ferrenberg and R.H. Swendsen, *Optimized Monte Carlo data analysis*, Phys. Rev. Lett. 63 (1989), pp. 1195–1198.
[18] G. Orkoulas, M.E. Fisher, and A.Z. Panagiotopoulos, *Precise simulation of criticality in asymmetric fluids*, Phys. Rev. E 63 (2001), pp. 051507-1–051507-14.
[19] R. Ren and G. Orkoulas, *Parallel Markov chain Monte Carlo simulations*, J. Chem. Phys. 126 (2007), pp. 211102-1–211102-4.
[20] M.E. Fisher and M.N. Barber, *Scaling theory for finite-size effects in the critical region*, Phys. Rev. Lett. 28 (1972), pp. 1516–1519.
[21] K. Binder, *Applications of Monte Carlo methods to statistical physics*, Rep. Prog. Phys. 60 (1997), pp. 487–559.
[22] M.E. Fisher, *The renormalization group in the theory of critical behavior*, Rev. Mod. Phys. 46 (1974), pp. 597–616.
[23] Y.C. Kim and M.E. Fisher, *Asymmetric fluid criticality. II. Finite-size scaling for simulations*, Phys. Rev. E 68 (2003), pp. 041506-1–041506-23.
[24] J.I. Siepmann, *A method for the direct calculation of chemical potentials for dense chain systems*, Mol. Phys. 70 (1990), pp. 1145–1158.
[25] D. Frenkel and B. Smit, *Unexpected length dependence of the solubility of chain molecules*, Mol. Phys. 75 (1992), pp. 983–988.
[26] J.J. de Pablo, M. Laso, and U.W. Suter, *Estimation of the chemical potential of chain molecules by simulation*, J. Chem. Phys. 96 (1992), pp. 6157–6162.
[27] G. Orkoulas and A.Z. Panagiotopoulos, *Free energy and phase equilibria for the restricted primitive model of ionic fluids from*

*Monte Carlo simulations*, J. Chem. Phys. 101 (1994), pp. 1452–1459.
[28] G. Orkoulas and A.Z. Panagiotopoulos, *Phase behavior of the restricted primitive model and square-well fluids from Monte Carlo simulations in the grand canonical ensemble*, J. Chem. Phys. 110 (1999), pp. 1581–1590.
[29] A.M. Ferrenberg and D.P. Landau, *Critical behavior of the three-dimensional Ising model: A high-resolution Monte Carlo study*, Phys. Rev. B 44 (1991), pp. 5081–5091.
[30] C. Predescu, M. Predescu, and C.V. Ciobanu, *The incomplete beta function law for parallel tempering sampling of classical canonical systems*, J. Chem. Phys. 120 (2004), pp. 4119–4128.
[31] N. Rathore, M. Chopra, and J.J. de Pablo, *Optimal allocation of replicas in parallel tempering simulations*, J. Chem. Phys. 122 (2005), pp. 024111-1–024111-8.
[32] A. Kone and D.A. Kofke, *Selection of temperature intervals for parallel-tempering simulations*, J. Chem. Phys. 122 (2005), pp. 206101-1–206101-2.